Performance of DS–CDMA with chip interleaving and frequency domain equalisation in a fading channel

D. Garg and F. Adachi

Abstract: Conventional time domain rake combining can be replaced by minimum mean square error frequency domain equalisation (MMSE–FDE) with much better performance in a frequency-selective fading channel, since the frequency selectivity of the channel is thoroughly exploited. Chip interleaving is a form of channel interleaving that improves the DS–CDMA performance by taking advantage of the time selectivity of the channel. The combined effect of chip interleaving and MMSE–FDE is evaluated. The theoretical analysis of uncoded BER performance in a frequency-selective Rayleigh fading channel is presented and confirmed by computer simulations. It is found that chip interleaving improves the performance for all channel conditions and that the chip interleaving gain increases with the increase in spreading factor *SF*. In addition, it is shown by computer simulations that chip interleaving is beneficial in the presence of turbo coding and antenna diversity as well.

1 Introduction

Recently, there have been tremendous demands for high-speed data transmissions in mobile communications. However, the hostile fading channel is a major obstacle to achieving high-speed data transmissions. The mobile communication channel is composed of many distinct propagation paths having different time delays, resulting in a frequency-selective fading channel [1]. Direct sequence code division multiple access (DS–CDMA) is used in cellular mobile communications systems for improving the performance of around a few Mbps transmissions [2]. DS–CDMA provides flexible data transmissions in a wide range of data rates by using orthogonal multicode multiplexing or changing the spreading factor. To exploit the frequency selectivity of the channel, time domain rake combining is used as a channel matched filter [3]. As the rate becomes faster, the number of distinguishable paths increases and the channel selectivity becomes stronger resulting in severe interpath interference (IPI). This produces severe intercode interference (ICI) when multicode transmission is utilised as in the downlink. Recently, in cellular mobile radio communications systems, much faster downlink access is required than uplink access. Therefore, reducing the ICI is an important issue. An effective way to reduce the ICI while exploiting the channel frequency selectivity and thus improve the BER performance, is to apply minimum mean square error (MMSE) frequency domain equalisation (FDE) to multicode DS–CDMA signal reception [4]. When FDE is used, the frequency selectivity of the channel is thoroughly exploited. It is shown in [5] that the use of MMSE–FDE provides a BER performance significantly better than that with rake combining in a frequency-selective fading channel.

The mobile channel is time- and frequency-selective. Chip interleaving is a form of channel interleaver that exploits the spreading process in DS–CDMA and thus benefits from the time selectivity of the channel. In [6], chip interleaving is proposed to improve the BER performance in a frequency-nonselective fading channel. Chip interleaving distributes the chips in time and transforms the transmission channel into a highly time-selective channel; the equivalent propagation channel gain seen after chip deinterleaving varies over one symbol interval. As a result, the time diversity effect is obtained and the received symbol energy varies less. In [7], chip interleaving has been applied to a multicode DS–CDMA system with rake combining. Multicode transmission relies on the fact that the channel stays constant over the symbol duration. Chip interleaving distributes the chips in time to ensure that the channel gain is different for the different chips. Hence, using chip interleaving degrades the multicode transmission performance because of the partial destruction of the code orthogonality property. Hence, in [7] MMSE time domain equalisation is introduced to partially restore orthogonality destruction. However, in a channel with more than four strong paths, the chip interleaved performance is worse than that without chip interleaving [7]. In this paper, we apply chip interleaving to multicode DS–CDMA with MMSE–FDE. In addition to frequency diversity gain due to MMSE–FDE, chip interleaving benefits from the channel's time selectivity. Using chip interleaving degrades the multicode transmission performance with time domain rake combining because of partial destruction of the code orthogonality property. However, when MMSE–FDE is applied, instead of time domain rake combining, the orthogonality is partially restored in addition to achieving frequency diversity.

Recently, multicarrier code division multiple access (MC–CDMA) [8, 9] based on orthogonal frequency division multiplexing (OFDM) has been attracting much attention and is under extensive study. In MC–CDMA, the data-modulated symbol to be transmitted is spread over a number of subcarriers using an orthogonal spreading

IEE Proceedings online no. 20045103
doi:10.1049/ip-com:20045103
Paper first received 6th July 2004 and in final revised form 9th April 2005

The authors are with Dept. of Electrical and Communications Engineering, Graduate School of Engineering, Tohoku University, Sendai, Japan
E-mail: adachi@ecei.tohoku.ac.jp

sequence defined in the frequency domain to obtain the frequency diversity effect. OFDM is a special case of MC–CDMA with a spreading factor of one. Chip interleaving (or frequency interleaving) can improve the performance of MC–CDMA systems as well. The performance of chip-interleaved DS–CDMA is compared with that of MC–CDMA.

2 Transmission system model

Figure 1 shows the equivalent lowpass transmission system model. The information sequence is turbo-coded and data-modulated. After multicode spreading, chip interleaving is performed and the signal transmitted after guard interval (GI) insertion; N_g-chip GI is inserted for every N_f chips, where N_f is the number of FFT points and N_g is a fraction of N_f. At the receiver with M receive antennas, the GI is removed and FFT is performed for each block of N_f chips received on each antenna. MMSE–FDE is carried out for each frequency component and after the signal components from different antennas are added, IFFT is performed followed by chip deinterelaving, multicode despreading, data demodulation and turbo decoding.

The chip interleaver/deinterleaver structure is shown in Fig. 2. It is a $N_f \times N_c$-block interleaver in which the chips are written row wise and read out column wise, N_c is chosen to be larger than SF. Hence, at the receiver, FFT is performed for the N_f chips belonging to N_f different symbols. After equalisation, the chips are deinterleaved with a block interleaver in which the chips are written column wise; the chips in an FDE block fall in one column. The chips are then read out row-by-row and despreading is carried out. The chips of a symbol are collected from different FDE blocks and, thus, time diversity gain can be attained in addition to frequency diversity due to MMSE–FDE.

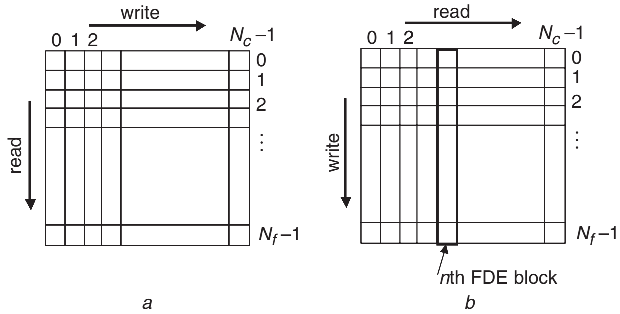

Fig. 2 *Chip interleaver/deinterleaver*
a Interleaver
b Deinterleaver

2.1 Transmit signal

The information sequence is turbo-coded and transformed into a data-modulated symbol sequence. Let the data-modulated symbol sequence length be $C \cdot K$. It is converted to C parallel streams $\{x_c(i);\ c = 0 \sim C-1,\ i = 0 \sim K-1\}$ by a serial-to-parallel (S/P) converter, each spread by the orthogonal code $\{c_{oc,c}(t);\ c = 0 \sim C-1, t = 0 \sim SF-1\}$, then added and further multiplied by the common scrambling code $\{c_{scr}(t)\}$. The resulting sequence is

$$s(t) = \sqrt{2P}\sum_{c=0}^{C-1} x_c(\lfloor t/SF \rfloor)c_{oc,c}(t \bmod SF)c_{scr}(t) \quad (1)$$

for $t = 0 \sim SF \cdot K - 1$, where P represents the transmit power per spreading code, C is the number of codes multiplexed, SF is the spreading factor, $\lfloor a \rfloor$ denotes the largest integer smaller than or equal to a and $|x_c(t)| = |c_{oc,c}(t)| = |c_{scr}(t)| = 1$. The orthogonal spreading sequences and the scramble sequence have the following characteristics:

$$\begin{cases} \dfrac{1}{SF}\displaystyle\sum_{t=0}^{SF-1} c_{oc,c}(t)c^*_{oc,c'}(t) = \delta(c-c') \\ E\left[c_{scr}(t)c^*_{scr}(\tau)\right] = \delta(t-\tau) \end{cases} \quad (2)$$

where $(\cdot)^*$ denotes the complex conjugate operation, $\delta(x)$ the delta function and $E[\cdot]$ the ensemble average operation. The resulting chip sequence is chip-interleaved, giving the sequence $\{s(t')\}$. After insertion of the N_g-sample GI for every block of N_f chips, the resultant GI-inserted,

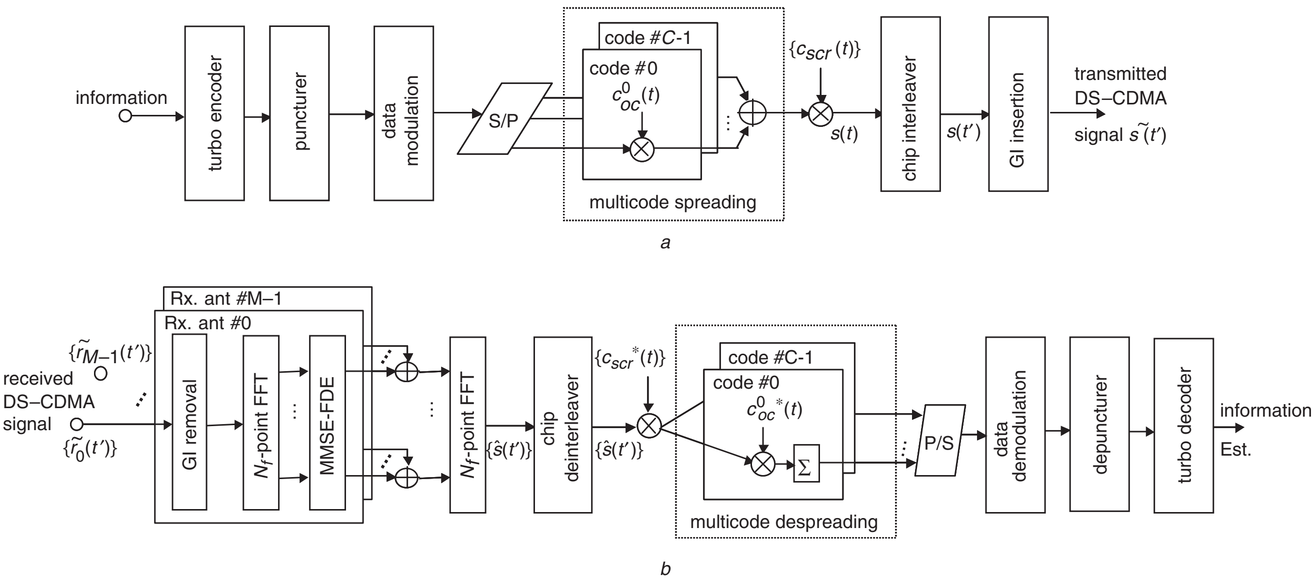

Fig. 1 *Transmission system model*
a Transmitter
b Receiver

interleaved multicode DS–CDMA signal $\tilde{s}(t')$ is transmitted over the propagation channel [4, 5].

2.2 Received signal

It is assumed that the propagation channel has L discrete paths having chip-spaced (or FFT sample-spaced) time delays and experiencing independent Rayleigh fading. M-branch antenna diversity reception is considered. The channel impulse response $h_m(\tau, n)$ associated with the mth antenna at the nth chip block with $(N_f + N_g)$ chips can be expressed as [10]

$$h_m(n) = \sum_{l=0}^{L-1} h_{m,l}(n)\delta(\tau - \tau_l) \quad (3)$$

where $h_{m,l}(n)$ and τ_l denote the complex-valued path gain and the time delay of the lth path, respectively, with

$$E\left[\sum_{l=0}^{L-1} |h_{m,l}(n)|^2\right] = 1$$

We have assumed a block fading where path gains stay constant during each block, but vary block-by-block. $\{h_{m,l}(n);\ l = 0 \sim L-1\}$ are independent zero-mean complex Gaussian processes.

The received signal at the mth antenna is sampled at the chip rate to obtain

$$\tilde{r}_m(t') = \sum_{l=0}^{L-1} h_{m,l}\left(\left\lfloor \frac{t'}{N_f + N_g}\right\rfloor\right)\tilde{s}(t' - \tau_l) + \eta_m(t') \quad (4)$$

for $t' = 0 \sim SF \cdot K(1 + N_g/N_f) - 1$ and $m = 0 \sim M-1$, where $\eta_m(t')$ is the additive white Gaussian noise (AWGN) process with zero mean and variance $2N_0/T_c$ (T_c is the chip length).

2.3 Frequency domain equalisation and chip deinterleaving

Ideal sampling timing is assumed. The N_g-sample GI is removed and N_f-point FFT is applied to each block of N_f chips to decompose the received signal into the N_f-frequency components. The kth frequency component for the nth block is

$$R_m(n, k) = \sum_{t'=nN_f}^{(n+1)N_f-1} \tilde{r}_m(t') \exp\left(-j2\pi k(t' \bmod N_f)/N_f\right)$$
$$= H_m(n, k)S(n, k) + \Pi_m(n, k) \quad (5)$$

for $k = 0 \sim N_f - 1$, $n = 0 \sim N_c - 1$, and $m = 0 \sim M-1$, where

$$\begin{cases} S(n, k) = \sum_{t'=nN_f}^{(n+1)N_f-1} s(t') \exp\left(-j2\pi k \frac{t'}{N_f}\right) \\ H_m(n, k) = \sum_{l=0}^{L-1} h_{m,l}(n) \exp\left(-j2\pi \frac{\tau_l}{N_f}\right) \\ \Pi_m(n, k) = \sum_{t'=nN_f}^{(n+1)N_f-1} \eta_m(t') \exp\left(-j2\pi k \frac{t'}{N_f}\right) \end{cases} \quad (6)$$

Here, $H_m(n, k)$ denotes the channel gain at the nth block's kth frequency component for the mth receive antenna. The frequency domain MMSE equalisation weight $w_m(n, k)$ for $R_m(n, k)$ is given by [5]

$$w_m(n, k) = \frac{H_m^*(n, k)}{\sum_{m=0}^{M-1} |H_m(n, k)|^2 + \left[\frac{C}{SF}\left(\frac{E_s}{N_0}\right)\right]^{-1}} \quad (7)$$

where $E_s = PT_cSF$ represents the average received signal energy per symbol.

After performing MMSE–FDE, the signal components from the different antennas are added to obtain

$$\hat{R}(n, k) = \sum_{m=0}^{M-1} w_m(n, k)R_m(n, k)$$
$$= \hat{H}(n, k)S(n, k) + \hat{\Pi}(n, k) \quad (8)$$

for $k = 0 \sim N_f - 1$, where $\hat{H}(n, k)$ and $\hat{\Pi}(n, k)$ are the equivalent channel gain and the noise due to AWGN, respectively, given by

$$\begin{cases} \hat{H}(n, k) = \sum_{m=0}^{M-1} H_m(n, k)w_m(n, k) \\ \hat{\Pi}(n, k) = \sum_{m=0}^{M-1} \Pi_m(n, k)w_m(n, k) \end{cases} \quad (9)$$

Then N_f-point IFFT is carried out to obtain the multicode DS–CDMA signal in the time domain

$$\hat{s}(t') = \frac{1}{N_f}\sum_{k=0}^{N_f-1} \hat{R}(n, k) \exp\left(j2\pi k \frac{t'}{N_f}\right)$$
$$= \left(\frac{1}{N_f}\sum_{k=0}^{N_f-1} \hat{H}(n, k)\right)s(t') + \frac{1}{N_f}\sum_{k=0}^{N_f-1} \hat{H}(n, k)$$
$$\times \left[\sum_{\substack{\tau=nN_f \\ \neq t'}}^{(n+1)N_f-1} s(\tau) \exp\left(j2\pi k \frac{t'-\tau}{N_f}\right)\right]$$
$$+ \frac{1}{N_f}\sum_{k=0}^{N_f-1} \hat{\Pi}(n, k) \exp\left(j2\pi k \frac{t'}{N_f}\right) \quad (10)$$

for $t' = nN_f \sim (n+1)N_f - 1$. The first term is the desired chip component, the second the ICI due to IPI and the third term the noise component. After the entire chip sequence is received, chip deinterleaving is performed giving the deinterleaved chip sequence $\{\hat{s}(t);\ t = 0 \sim SF \cdot K - 1\}$.

2.4 Despreading

After chip deinterleaving, multicode despreading is carried out to obtain

$$\hat{x}_c(i) = \frac{1}{SF}\sum_{t=iSF}^{(i+1)SF-1} \hat{s}(t)\{c_{oc,c}(t \bmod SF)c_{scr}(t)\}^*$$
$$= \sqrt{2P}\left[\frac{1}{SF}\sum_{t=iSF}^{(i+1)SF-1}\left(\frac{1}{N_f}\sum_{k=0}^{N_f-1} \hat{H}(n', k)\right)\right]d_c(i)$$
$$+ \mu_{ICI}(i) + \mu_{AWGN}(i) \quad (11)$$

for $c = 0 \sim C - 1$, and $i = 0 \sim K - 1$ and $n' = t \bmod N_c$ (N_c is the number of columns in the chip interleaver taken as

$$N_c = \frac{SF \times K}{N_f}$$

$\mu_{ICI}(i)$ and $\mu_{AWGN}(i)$ are the ICI and noise due to AWGN, given by

$$\begin{cases} \mu_{ICI}(i) = \frac{1}{SF}\sum_{t=iSF}^{(i+1)SF-1}\{c_{oc,c}(t \bmod SF)c_{scr}(t)\}^* \\ \quad \times\left(\frac{1}{N_f}\sum_{k=0}^{N_f-1}\hat{H}(n',k)\right)\left[\sum_{\substack{\tau=n'N_f \\ \neq t}}^{(n'+1)N_f-1} s(\tau)\exp\left(j2\pi k\frac{t'-\tau}{N_f}\right)\right] \\ \mu_{AWGN}(i) = \frac{1}{SF}\sum_{t=iSF}^{(i+1)SF-1}\{c_{oc,c}(t \bmod SF)c_{scr}(k)\}^* \\ \quad \times\left\{\frac{1}{N_f}\sum_{k=0}^{N_f-1}\hat{\Pi}(n',k)\exp\left(j2\pi k\frac{t}{N_f}\right)\right\} \end{cases} \tag{12}$$

Since the chip interleaver is designed such that the chips belonging to a symbol fall in different FFT blocks (see Fig. 2), the equivalent channel gain $\hat{H}(n',k)$ for each chip is different. It can be observed from (11) that as a result of chip deinterleaving, the equivalent channel gain for each symbol is

$$\left[\frac{1}{SF}\sum_{t=iSF}^{(i+1)SF-1}\left(\frac{1}{N_f}\sum_{k=0}^{N_f-1}\hat{H}(n',k)\right)\right]$$

with $n' = t \bmod N_c$ and is dependent on SF; the equivalent channel gain over SF different FFT intervals are averaged, thereby achieving time diversity effect as in a frequency nonselective channel [6].

The soft values $\{\hat{x}_c(i)\}$ are parallel-to-serial (P/S) converted for data demodulation and then turbo decoded.

3 BER analysis

In this Section, we derive the conditional BER based on Gaussian approximation of ICI, and then numerically evaluate the average BER performance. It can be understood from (11) that the despreader output $\hat{x}_c(i)$ is a random variable with mean

$$\sqrt{2P}\left[\frac{1}{SF}\sum_{t=iSF}^{(i+1)SF-1}\left(\frac{1}{N_f}\sum_{k=0}^{N_f-1}\hat{H}(n',k)\right)\right]d_c(i)$$

where $n' = t \bmod N_c$. Since the scramble sequence is used to make the resultant multicode DS–CDMA signal white-noise-like, i.e. $E[s(t)s^*(\tau)] = 2PC\delta(t-\tau)$, μ_{ICI} can be approximated as a zero-mean complex Gaussian noise. The sum of μ_{ICI} and μ_{AWGN} can be treated as a new zero-mean complex Gaussian noise μ. The variance of μ is the sum of those of μ_{ICI} and μ_{AWGN}:

$$2\sigma_\mu^2 = E\left[|\mu|^2\right] = 2\sigma_{ICI}^2 + 2\sigma_{AWGN}^2 \tag{13}$$

where, from the Appendix (Section 7.1)

$$\begin{cases} \sigma_{ICI}^2 = \frac{1}{2}E\left[|\mu_{ICI}|^2\right] \\ \quad = P\frac{C}{SF^2}\left\{\frac{1}{N_f}\sum_{t=iSF}^{(i+1)SF-1}\sum_{k=0}^{N_f-1}\left|\hat{H}(n',k)\right|^2 - \left|\frac{1}{N_f}\sum_{t=iSF}^{(i+1)SF-1}\sum_{k=0}^{N_f-1}\hat{H}(n',k)\right|^2\right\} \\ \sigma_{AWGN}^2 = \frac{1}{2}E\left[|\mu_{AWGN}|^2\right] \\ \quad = \frac{N_0}{T_c}\frac{1}{SF^2}\left(\frac{1}{N_f}\sum_{t=iSF}^{(i+1)SF-1}\sum_{k=0}^{N_f-1}\sum_{m=0}^{M-1}|w_m(n',k)|^2\right) \end{cases} \tag{14}$$

for the given set of $\{H_m(n,k)$ and $w_m(n,k)$; $k = 0 \sim N_f - 1$ and $m = 0 \sim M\text{-}1\}$. Therefore, we have

$$\sigma_\mu^2 = \frac{N_0}{T_c}\frac{1}{SF^2}\left[\frac{1}{N_f}\sum_{t=iSF}^{(i+1)SF-1}\sum_{k=0}^{N_f-1}\sum_{m=0}^{M-1}|w_m(n',k)|^2 + \left(\frac{C}{SF}\frac{E_s}{N_0}\right)\left\{\frac{1}{N_f}\sum_{t=iSF}^{(i+1)SF-1}\sum_{k=0}^{N_f-1}\left|\hat{H}(n',k)\right|^2 - \left|\frac{1}{N_f}\sum_{t=iSF}^{(i+1)SF-1}\sum_{k=0}^{N_f-1}\hat{H}(n',k)\right|^2\right\}\right] \tag{15}$$

We assume all '1' transmission without loss of generality and quaternary phase shift keying (QPSK) data modulation. Since the ICI can be assumed to be circularly symmetric, the conditional BER for the given set of $\{H_m(n,k)$; $k = 0 \sim N_f - 1$ and $m = 0 \sim M\text{-}1\}$ can be expressed as [11]

$$\begin{aligned} p_b\left(\frac{E_s}{N_0}, \{H_m(n,k)\}\right) &= \frac{1}{2}\text{Prob}[\text{Re}[\hat{x}_c(n)] < 0 | \{H_m(n,k)\}] \\ &\quad + \frac{1}{2}\text{Prob}[\text{Im}[\hat{x}_c(n)] < 0 | \{H_m(n,k)\}] \\ &= \frac{1}{2}erfc\left[\sqrt{\frac{1}{4}\gamma\left(\frac{E_s}{N_0}, \{H_m(n,k)\}\right)}\right] \end{aligned} \tag{16}$$

where $erfc[x] = (2/\sqrt{\pi})\int_x^\infty \exp(-t^2)dt$ is the complementary error function, and $\gamma(E_s/N_0, \{H_m(n,k\})$ is the conditional signal-to-interference plus noise power ratio (SINR) given by

$$\gamma\left(\frac{E_s}{N_0}, \{H_m(n,k)\}\right) = \frac{2P\left|\frac{1}{SF}\sum_{t=iSF}^{(i+1)SF-1}\left(\frac{1}{N_f}\sum_{k=0}^{N_f-1}\hat{H}(n',k)\right)\right|^2}{\sigma_\mu^2} \tag{17}$$

The average BER can be numerically evaluated by averaging Eq. (17) over $\{H_m(n,k)$; $k = 0 \sim N_f - 1$ and $m = 0 \sim M-1\}$:

$$P_b\left(\frac{E_s}{N_0}\right) = \int\cdots\int\frac{1}{2}erfc\left[\sqrt{\frac{1}{4}\gamma\left(\frac{E_s}{N_0}, \{H_m(n,k)\}\right)}\right] \times p(\{H_m(n,k)\})\prod_{m,k}dH_m(n,k) \tag{18}$$

where $p(\{H_m(n,k)\})$ is the joint probability density function (pdf) of $\{H_m(n,k)$; $k = 0 \sim N_f - 1$ and $m = 0 \sim M-1\}$.

4 Numerical and simulation results

The uncoded case is considered first. The theoretical BER performance using the conditional BER expression derived in Section 3 is numerically evaluated and then its validity confirmed by computer simulations. Next, the evaluation is done for the coded case. Since the BER analysis of the coded case is quite difficult, if not impossible, we only present the computer simulation results to show the performance improvements achievable by the joint use of MMSE–FDE and chip interleaving.

The simulation conditions are summarised in Table 1. For numerical and simulation purposes, we assume a frequency-selective channel having a 16-path ($L = 16$) exponential power delay profile with decay factor α dB and a time delay separation of 1 chip between adjacent

Table 1: Simulation conditions

Turbo code	Encoder	(13, 15) RSC
	Decoder	Log-MAP eight iterations
Data modulation	QPSK	
Spreading codes	Short orthogonal codes and long PN code	
Chip interleaver	256 × 256 block interleaver	
FFT/IFFT points	$N_f = 256$	
Guard interval	$N_g = 32$	
Channel	16-path Rayleigh fading	

paths (i.e. $\tau_l = l$). Data modulation and spreading modulation are taken to be QPSK and BPSK, respectively. The number N_f of FFT and IFFT points is taken to be 256. The chip interleaver is a 256×256 ($N_f = N_c = 256$)-block interleaver. For the coded case, turbo coding is applied. A rate-1/3 turbo encoder with a constraint length of four is punctured to obtain 1/2 and 3/4 rate code. The decoder is a log-MAP decoder with eight iterations. Ideal channel estimation is assumed.

The chip-interleaved performance is compared with that without chip interleaving. When chip interleaving is not applied, a bit interleaver of the same size is inserted after turbo coding and puncturing in the transmitter and a complementary bit deinterleaver is placed before turbo decoding at the receiver.

4.1 Uncoded case

Figure 3 plots the uncoded theoretical average BER performance (solid and dotted curves) as a function of the average received signal energy per information bit to the noise power spectrum density ratio (E_b/N_0) with the decay factor α as a parameter for a normalised maximum Doppler frequency $f_D T_{blk}$ of 0.01, where $T_{blk} = (N_f + N_g)T_c$. $SF = C = 256$ is assumed. $\alpha = 0$ dB corresponds to a uniform power delay profile, resulting in a highly frequency-selective channel. As the value of α decreases the channel's frequency-selectivity increases. It is seen that as the value of α decreases, the BER improves because of the increase in the frequency diversity effect. Chip interleaving gives a better performance than no chip interleaving for all values of α. A gain of 8 dB is seen for a $\text{BER} = 10^{-4}$ when $\alpha = 12$ dB.

As said earlier, chip interleaving converts the channel into a highly time-selective channel and hence the BER performance improves. With higher frequency selectivity, the orthogonality among the different codes is destroyed. However, the use of MMSE–FDE, performed for each frequency component, provides a good trade-off between orthogonality restoration and noise enhancement, and so the BER performance is seen to be even better with chip interleaving. For larger values of α, where the frequency diversity is less, chip interleaving gain is higher and vice versa. With chip interleaving, the performance dependence on channel condition is reduced. For an average BER of 10^{-4}, the required average received E_b/N_0 reduces by only 3.5 dB when α changes from 12 dB to 0 dB in contrast to the 9.5 dB reduction in E_b/N_0 when chip interleaving is not applied.

The time diversity gain introduced by the chip interleaver is directly related to the fading rate; the gain is higher for fast fading and vise versa. Figure 4 plots the theoretical BER as a function of average E_b/N_0 with $f_D T_{blk}$ as a parameter. It is seen that chip interleaving reduces the BER for all values of $f_D T_{blk}$. However, without chip interleaving, the BER performance is the same for all values of $f_D T_{blk}$. The BER with chip interleaving improves with the increase in the fading rate owing to the increased time diversity effect achieved by chip interleaving. $f_D T_{blk}$ is about 0.01 for a carrier frequency of 5 GHz and a mobile velocity of 70 km/hr when the data rate is 10 Mbps; $f_D T_{blk}$ decreases with the increase in data rate or decrease in the mobile velocity. With chip interleaving, the required average E_b/N_0 for a $\text{BER} = 10^{-4}$ is about 4 dB less when $f_D T_{blk} = 0.01$, compared to the case without chip interleaving.

Chip interleaving scatters the chips belonging to a symbol further apart in time and attains a time diversity gain when the chips are despread; hence the spreading factor SF becomes an important parameter. Below, the dependence of chip interleaving gain on the SF is evaluated. Figure 5 plots

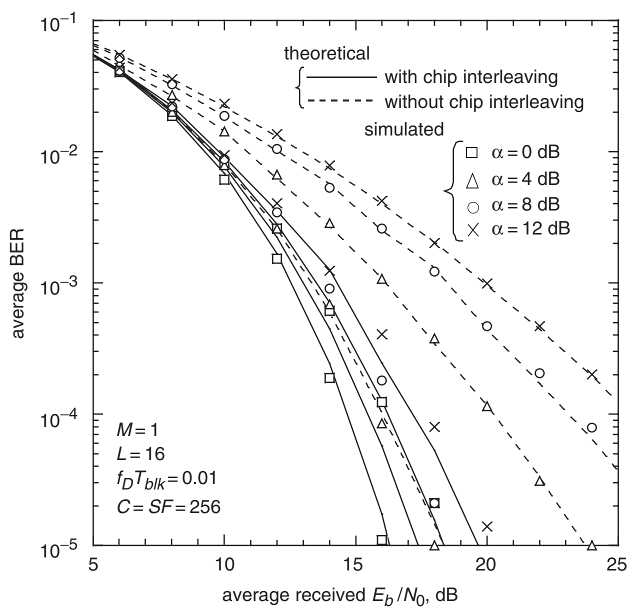

Fig. 3 *Uncoded BER performance with and without chip interleaving for $SF = C = 256$*

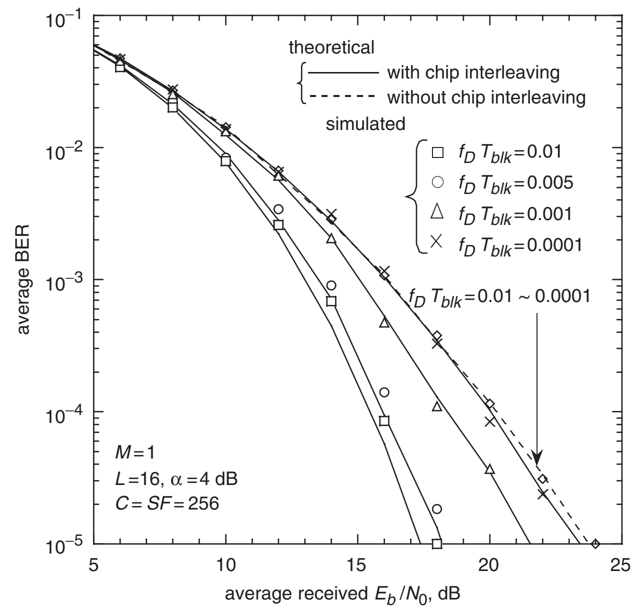

Fig. 4 *Uncoded BER performance with and without chip interleaving with $f_D T_{blk}$ as a parameter*

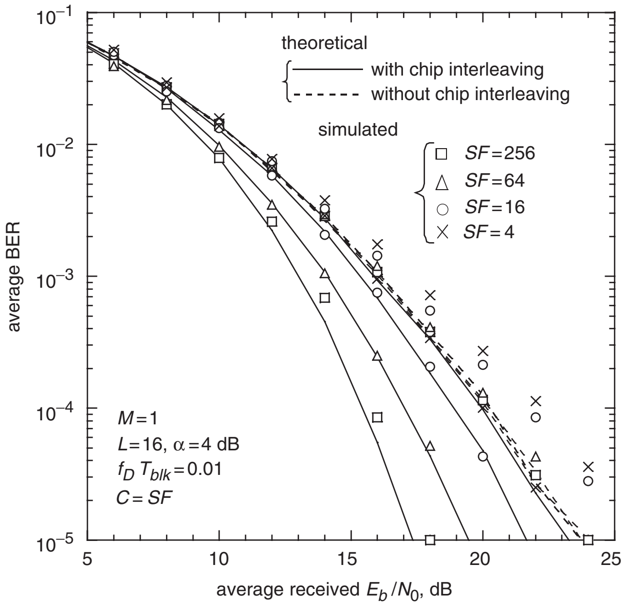

Fig. 5 *Uncoded BER performance with and without chip interleaving with SF as a parameter*

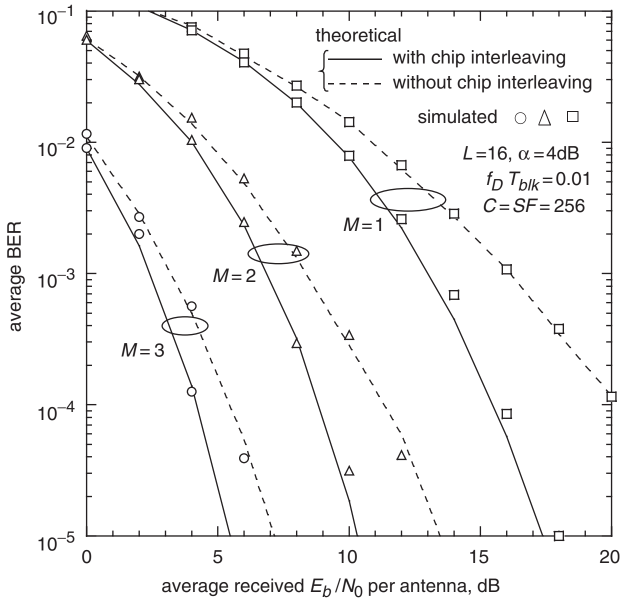

Fig. 6 *Uncoded BER performance with and without chip interleaving for antenna diversity reception*

the uncoded theoretical average BER as a function of average received E_b/N_0 with *SF* as a parameter when $\alpha = 4$ dB. In DS–CDMA, since each symbol is spread over the entire bandwidth, the frequency diversity is not sensitive to the value of *SF* [12]. In addition to the frequency diversity effect, chip interleaving achieves a time diversity gain as the chips in a symbol are distributed in time. From Fig. 5, we see that with chip interleaving, the BER performance improves as *SF* increases. This is because as *SF* increases, the chips are spread further apart in time, and hence there is less correlation among the channel gains experienced by the chips belonging to the same symbol. With larger *SF*, the chip interleaving gain is larger; when $SF = 4$ (256), about 2 dB (4 dB) improvement is seen in the average received E_b/N_0 required for a BER $= 10^{-4}$.

Antenna diversity is a well known technique to improve the transmission performance. An interesting question arises as to whether chip interleaving is beneficial in the presence of antenna diversity or not; and if so, to what extent. Figure 6 plots the uncoded average theoretical BER performance with and without chip when $f_D T_{blk} = 0.01$, $\alpha = 4$ dB and $SF = C = 256$. It is seen that even for $M = 2$, chip interleaving reduces the average required E_b/N_0 for a BER of 10^{-4} by about 2 dB. However, as the number of antennas increases, the chip interleaving gain decreases.

Also plotted in Figs. 3–6 are the computer simulation results. A fairly good agreement between the theoretical and simulation results is seen. This confirms the validity of the theoretical analysis presented in Section 3.

4.2 Turbo-coded case

Only the simulation results are presented here. Turbo coding gain in the presence of chip interleaving and bit interleaving are compared for $SF = C = 256$ in Figs. 7*a* and 7*b* when $\alpha = 4$ dB and 12 dB, respectively. A rate 1/3 turbo

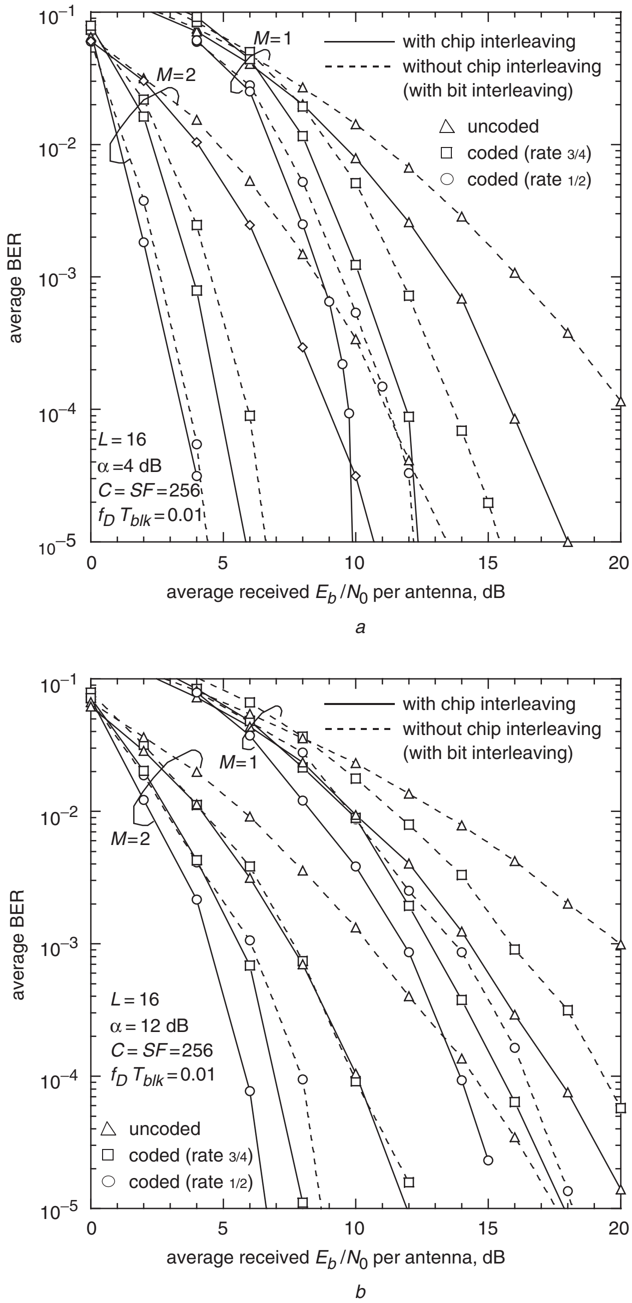

Fig. 7 *Turbo-coded BER performance*
a $\alpha = 4$ dB
b $\alpha = 12$ dB

code is punctured to get rate 1/2 and rate 3/4 turbo codes. It is seen that the BER performance with chip interleaving is better than that with bit interleaving for both $M=1$ and 2. Bit interleaving distributes the bits in time and hence improves the error correction capability of the channel coding, which in our case is turbo coding. For an uncoded system, the presence of bit interleaving makes no difference in the performance. However, chip interleaving changes the received signal statistics and improves the BER performance even when there is no channel coding applied as already discussed in Section 4.1. When $\alpha = 12$ dB and $M=1$, using chip interleaving instead of bit interleaving reduces the required E_b/N_0 for a BER $= 10^{-4}$ by 3 dB and 2.5 dB for rate 3/4 and 1/2 code, respectively. It is seen that even in the presence of antenna diversity, chip interleaved BER is better than that with bit interleaving. The chip interleaving gain is larger for $\alpha = 12$ dB and when the coding rate is 3/4.

4.3 Comparison with chip interleaved MC–CDMA

In MC–CDMA, the data-modulated symbol to be transmitted is spread over a number of subcarriers using an orthogonal spreading sequence defined in the frequency domain to obtain the frequency diversity effect. The MC–CDMA transmission system model is similar to that of DS–CDMA. The code-multiplexing order for MC–CDMA is also taken to be C. An introduction of N_f-point IFFT between the chip interleaver and the GI insertion in Fig. 1*a* gives the MC–CDMA transmitter. Replacing N_f-point IFFT by a P/S converter in Fig. 1*b* gives the MC–CDMA receiver. If the same $N_f \times N_c$-block interleaver as for DS–CDMA is used, the chips belonging to a symbol are spread over different FFT blocks but the same subcarrier. Therefore, time diversity gain will be obtained but there will be no frequency diversity gain. So, in order to attain the frequency diversity gain, N_f elements in each column of the chip interleaver are further interleaved (by doing so, the chips belonging to a symbol will be transmitted on different subcarriers). The chip interleaved MC–CDMA signal obtained by performing N_f-point IFFT is transmitted after the GI insertion. At the receiver, deinterleaving is carried out after performing N_f-point FFT and MMSE–FDE, and is followed by multicode despreading, P/S conversion, and data demodulation. Figure 8 compares the average BER performances of chip interleaved DS–CDMA and MC–CDMA when the turbo coding rate is 1/2. $SF(=N_f)=256$ and full load condition $C=SF$ is assumed. It has been found [12] that when $SF=N_f$, DS–CDMA and MC–CDMA provide the same BER performance. It can be seen from Fig. 8 that even with chip interleaving, DS–CDMA with MMSE–FDE provides the same BER performance as MC–CDMA.

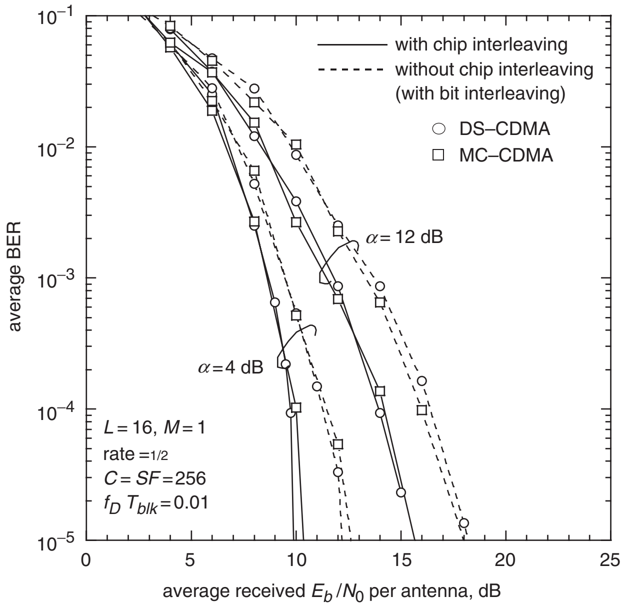

Fig. 8 *Performance comparison of chip-interleaved DS–CDMA and MC–CDMA*

5 Conclusions

Chip interleaving and MMSE–FDE were jointly used in multicode DS–CDMA to take advantage of the time- and frequency-selectivity of the channel. MMSE–FDE provides a high frequency diversity gain in a frequency-selective channel as each symbol is spread over the entire bandwidth available and equalisation is performed in the frequency domain. Chip interleaving benefits from the time-selectivity of the channel by distributing the chips in time. The uncoded BER performance analysis was presented to show that chip interleaving improves the performance for all channel conditions and that the chip interleaving gain is larger for higher spreading factor SF. The theoretical analysis was confirmed by computer simulation. Performance evaluation was done by computer simulation for the turbo-coded case as well. It was found that chip interleaving is effective in the presence of turbo coding and antenna diversity as well. Also presented was the performance comparison between chip-interleaved DS–CDMA and MC–CDMA. It was found that when $SF=N_f$, chip-interleaved DS–CDMA achieves the same BER performance as chip-interleaved MC–CDMA. However, when SF is lower than N_f, the MC–CDMA performance is dependent on SF [13]. The detailed study of chip-interleaved MC–CDMA is left as an interesting future study.

6 References

1 Jakes, W.C., Jr., (Ed.): 'Microwave mobile communications' (Wiley, New York, 1974)
2 Adachi, F., Sawahashi, M., and Suda, H.: 'Wideband DS-CDMA for next generation mobile communications systems', *IEEE Commun. Mag.*, 1998, **36**, pp. 56–69
3 Proakis, J.G.: 'Digital communications' (McGraw Hill, Singapore, 2001)
4 Adachi, F., Sao, T., and Itagaki, T.: 'Performance of multicode DS-CDMA using frequency domain equalization in a frequency selective fading channel', *Electron. Lett.*, 2003, **39**, (2), pp. 239–241
5 Itagaki, T., and Adachi, F.: 'Joint frequency domain equalization and antenna diversity combining for orthogonal multicode DS-CDMA signal transmissions in a frequency selective fading channel'. Proc. WPMC03, Yokosuka, Japan, Oct. 2003, Vol. 1, pp. 285–289
6 Garg, D., and Adachi, F.: 'Chip interleaved turbo codes for DS-CDMA mobile radio in a fading channel', *Electron. Lett.*, 2002, **38**, (13), pp. 642–644
7 Itagaki, T., Sao, T., Garg, D., and Adachi, F.: 'Chip interleaved miulticode DS-CDMA and MMSEC in a fading channel', *IEICE Trans. Commun.*, 2004, **E87-B**, (1), pp. 79–87
8 Chouly, A., Brajal, A., and Jourdan, S.: 'Orthogonal multicarrier techniques applied to direct sequence spread spectrum CDMA system'. Proc. IEEE Globecom'93, Nov. 1993, pp. 1723–1728
9 Hara, S., and Prasad, R.: 'Overview of multicarrier CDMA', *IEEE Commun. Mag.*, 1997, **35**, (12), pp. 126–133
10 Kchao, C., and Stuber, G.L.: 'Analysis of a direct-sequence spread-spectrum cellular radio system', *IEEE Trans. Commun.*, 1993, **41**, pp. 1507–1516
11 Proakis, J.G.: 'Digital communications' (McGraw Hill, Singapore, 2001)
12 Adachi, F., and Takeda, K.: 'Bit error rate analysis of DS–CDMA with joint frequency-domain equalization and antenna diversity combining', *IEICE Trans. Commun.*, 2004, **E87-B**, (10), pp. 2991–3002
13 Garg, D., and Adachi, F.: 'Diversity-coding-orthogonality trade-off for coded MC–CDMA with high level modulation', *IEICE Trans. Commun.*, 2005, **E88-B**, (1), pp. 76–83

7 Appendix

7.1 Derivation of σ^2_{ICI} and σ^2_{AWGN}

For simplicity, we express $c_{oc,c}(k \bmod SF)c_{scr}(k)$ as $c(k)$. Since $E[c(t)c^*(\tau)] = \delta(t-\tau)$, we have

$$\sigma^2_{ICI} = \frac{1}{2}\frac{1}{SF^2N_f^2}\sum_{t=iSF}^{(i+1)SF-1}\sum_{k=0}^{N_f-1}\sum_{k'=0}^{N_f-1}\hat{H}(n',k)\hat{H}^*(n',k') \times \left[\sum_{\substack{\tau=0\\ \neq t}}^{N_f-1}\sum_{\substack{\tau'=0\\ \neq t}}^{N_f-1}E[s(\tau)s^*(\tau')]\exp\left(j2\pi k\frac{t-\tau}{N_f} - j2\pi k'\frac{t-\tau'}{N_f}\right)\right] \quad (19)$$

where $n' = t \bmod N_c$ (N_c is the number of columns in the chip interleaver). The DS–CDMA signal using the scramble sequence together with orthogonal spreading sequences is white-noise-like and hence, $E[s(\tau)s^*(\tau')] = 2PC\delta(\tau-\tau')$. Therefore, (19) becomes

$$\begin{aligned}\sigma^2_{ICI} &= P\frac{C}{SF^2N_f^2}\sum_{t=iSF}^{(i+1)SF-1}\sum_{k=0}^{N_f-1}\sum_{k'=0}^{N_f-1}\hat{H}(n',k)\hat{H}^*(n',k') \times \left[\sum_{\substack{\tau=0\\ \neq t}}^{N_f-1}\exp\left(j2\pi(k-k')\frac{t-\tau}{N_f}\right)\right]\\ &= P\frac{C}{SF^2N_f^2}\sum_{t=iSF}^{(i+1)SF-1}\sum_{k=0}^{N_f-1}\sum_{k'=0}^{N_f-1}\hat{H}(n',k)\hat{H}^*(n',k') \times \left[\sum_{\tau=0}^{N_f-1}\exp\left(j2\pi(k-k')\frac{t-\tau}{N_f}\right)-1\right]\end{aligned} \quad (20)$$

Since

$$\sum_{\tau=0}^{N_f-1}\exp\left(j2\pi(k-k')\frac{t-\tau}{N_f}\right) = N_f\delta(k-k') \quad (21)$$

we obtain

$$\begin{aligned}\sigma^2_{ICI} &= P\frac{C}{SF^2}\frac{1}{N_f^2}\sum_{t=iSF}^{(i+1)SF-1}\sum_{k=0}^{N_f-1}\sum_{k'=0}^{N_f-1}\hat{H}(n',k)\hat{H}^* \times (n',k')\left[N_f\delta(k-k')-1\right]\\ &= P\frac{C}{SF^2}\left[\frac{1}{N_f}\sum_{t=iSF}^{(i+1)SF-1}\sum_{k=0}^{N_f-1}\left|\hat{H}(n',k)\right|^2 - \left|\frac{1}{N_f}\sum_{t=iSF}^{(i+1)SF-1}\sum_{k=0}^{N_f-1}\hat{H}(n',k)\right|^2\right]\end{aligned} \quad (22)$$

Next, we obtain σ^2_{AWGN}. Since $E[c(t)c^*(\tau)] = \delta(t-\tau)$, we have

$$\sigma^2_{AWGN} = \frac{1}{2}\frac{1}{SF^2N_f^2}\sum_{t=nSF}^{(n+1)SF-1}\sum_{k=0}^{N_f-1} \times \sum_{k'=0}^{N_f-1}E\left[\hat{\Pi}(n',k)\hat{\Pi}^*(n',k')\right]\exp\left(j2\pi(k-k')\frac{t}{N_f}\right) \quad (23)$$

Since $\{\Pi_m(n', k);\ m=0\sim M-1$ and $k=0\sim N_f-1\}$ are independent and zero-mean complex Gaussian variables having a variance of $2(N_0/T_c)N_f$, $\{\hat{\Pi}_{n'}(k);\ k=0\sim N_f-1\}$ are also independent and zero-mean complex Gaussian variables and, thus, we have

$$\sigma^2_{AWGN} = \frac{N_0}{T_c}\frac{1}{SF^2}\left(\frac{1}{N_f}\sum_{t=iSF}^{(i+1)SF-1}\sum_{k=0}^{N_f-1}\sum_{m=0}^{M-1}|w_m(n',k)|^2\right) \quad (24)$$